Title
Adult living donor liver imaging

Journal
Diagnostic and Interventional Radiology, 22(3)

ISSN
0998-433X

Authors
Cai, Larry
Yeh, Benjamin M
Westphalen, Antonio C
et al.

Publication Date
2016-05-03

DOI
10.5152/dir.2016.15323

Peer reviewed

Diagn Interv Radiol 2016; 22:207–214

ABDOMINAL IMAGING

REVIEW

Adult living donor liver imaging

Larry Cai
Benjamin M. Yeh
Antonio C. Westphalen
John P. Roberts
Zhen J. Wang

ABSTRACT

Adult living donor liver transplantation (LDLT) is increasingly used for the treatment of end-stage liver disease. The three most commonly harvested grafts for LDLT are left lateral segment, left lobe, and right lobe grafts. The left lateral segment graft, which includes Couinaud's segments II and III, is usually used for pediatric recipients or small size recipients. Most of the adult recipients need either a left or a right lobe graft. Whether a left or right lobe graft should be harvested from the donors depends on estimated graft and donor remnant liver volume, as well as biliary and vascular anatomy. Detailed preoperative assessment of the potential donor liver volumetrics, biliary and vascular anatomy, and liver parenchyma is vital to minimize risks to the donors and maximize benefits to the recipients. Computed tomography (CT) and magnetic resonance imaging (MRI) are currently the imaging modalities of choice in the preoperative evaluation of potential donors. This review provides an overview of key surgical considerations in LDLT that the radiologists must be aware of, and imaging findings on CT and MRI that the radiologists must convey to the surgeons when evaluating potential donors for LDLT.

Liver transplantation is the treatment of choice for end-stage liver disease (ESLD), such as that from alcoholic cirrhosis or viral hepatitis. The demand for donor livers is increasing, outstripping the available supply and creating a long waiting list of patients with ESLD, many of whom die while on the waiting list. Increasingly, living donor liver transplantation (LDLT) is seen as a viable alternative to deceased donor liver transplantation to increase the supply of available donor livers. Studies of LDLT have shown acceptable results in terms of short-term survival and graft outcomes compared with deceased donor liver transplantation with full size organ (1) and long-term donor quality of life (2). In the nine-center adult-to-adult living donor liver transplantation cohort study (A2ALL), one-year graft survival was 81% (3) and most living donors maintained an above average health-related quality of life at 11 years postoperatively (4). In addition, recent advancements in surgical techniques and presurgical evaluation and preparation have continued to improve outcomes (5).

LDLT is a major surgical undertaking. The healthy donor is subjected to a hemihepatectomy, a surgical procedure with significant risks, without apparent medical benefits to the donor. Studies have shown that living liver donors in the United States have a perioperative risk of mortality of 1.7 per 1000 donors (6), from causes including sepsis and acute liver failure. In addition, numerous other complications can occur after donation, including biliary leaks or stricture, and vascular thrombosis. Thus, careful evaluation and selection of the donors is mandatory to minimize the risks to the donors, as well as to maximize the benefits to the recipients. Preoperative imaging (computed tomography, CT; magnetic resonance imaging, MRI) plays a key role in the evaluation of donors by depicting biliary and hepatic vascular anatomy, liver volumetrics, and parenchymal disease, information that is key to safe LDLT. This review provides an overview of key surgical considerations in LDLT that the radiologists must be aware of, and imaging findings on CT and MRI that the radiologists must convey to the surgeons when evaluating potential donors for LDLT.

Types of LDLT and surgical considerations

The three most commonly harvested grafts for LDLT are left lateral segment, left lobe, and right lobe grafts. The left lateral segment graft, which includes the Couinaud's segments II and III, is usually used for pediatric recipients or small size recipients. Most of the

From the Departments of Radiology (L.C., B.M.Y., A.C.W., Z.J.W. ✉ *Jane.Wang@ucsf.edu*) and Surgery (J.P.R.) University of California, San Francisco, CA, USA.

Received 16 July 2015; revision requested 15 August 2015; revision received 29 August 2015; accepted 2 September 2015.

Published online 24 February 2016.
DOI 10.5152/dir.2016.15323

adult recipients need either a left or a right lobe graft. Whether a left or right lobe graft should be harvested from the donors depends on estimated graft and donor remnant liver volume, as well as biliary and vascular anatomy. Typically, the hemihepatectomy plane is 1 cm to the right of the middle hepatic vein (MHV), along Cantlie's line, running from the gallbladder fossa to the inferior vena cava (IVC) (Fig. 1). Left hepatectomy (segments II–IV) in the donors usually involves harvesting of the MHV to obtain a reasonably large graft volume and to maintain good graft viability. Right hepatectomy (segments V–VIII) can be performed in the donors if the donor's left lobe volume is greater than 30% of total hepatic volume. Right lobe grafts are often harvested without the MHV trunk. Such grafts are at increased risk for congestion of the right paramedian sector, especially if there are large branches draining the right lobe of the liver into the MHV, with subsequent graft dysfunction. To minimize such complications, MHV drainage to recipient IVC may be reconstructed with vascular grafts (7). The caudate lobe usually remains in the donor because it directly drains into the IVC.

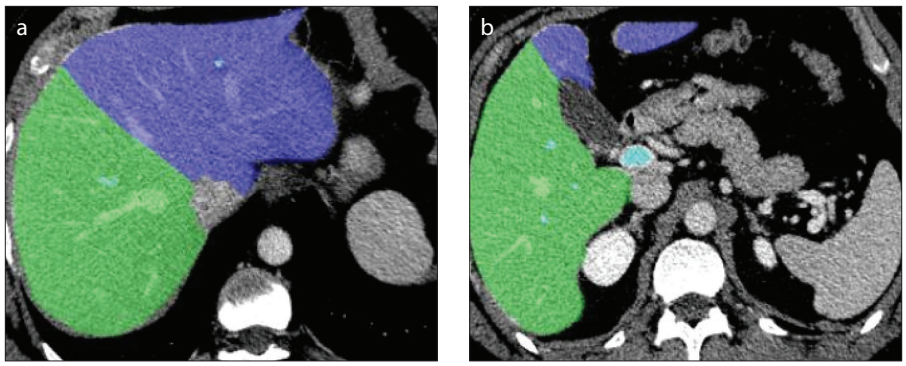

Figure 1. a, b. Axial contrast-enhanced CT through the liver **(a, b)** demonstrates the hemi-hepatectomy plane, separating the left *(purple)* and right *(green)* lobes of the liver. This plane runs 1 cm to the right of the middle hepatic vein, and connects the gallbladder fossa and the IVC.

Living liver donor imaging

Preoperative imaging provides noninvasive assessment of liver anatomy and possible pathology in potential donors in order to identify those not suitable for donation and to allow for preoperative planning. In a recent retrospective study of 159 liver donor candidates, 61 (38%) were excluded based on CT imaging findings. Of these patients, 66% were excluded due to inadequate liver volume, 23% were excluded due to vascular or biliary variants, and 8% were excluded due to steatosis (8).

CT and MRI are the main modalities for the preoperative assessment of potential living liver donors. The CT protocol for donors at our institution includes unenhanced CT followed by multiphase contrast-enhanced CT. For the unenhanced CT, a single slice of 5 mm through the mid-liver and spleen is obtained to assess for fatty liver. After intravenous injection of 120–150 mL of iodinated contrast material with a concentration of 350 mg iodine/mL at a rate of 4–5 mL per second, 1.25 mm slice thickness arterial and portal venous phase CT of the abdomen is acquired next to evaluate for hepatic vasculature and parenchyma. CT cholangiography can be performed to assess biliary anatomy. First, to reduce the risk of allergic reaction, 25 mg of diphenhydramine (Benadryl; Pfizer) is administered intravenously. The cholangiographic contrast, 20 mL of 52% iodipamide meglumin (Cholografin; Bracco Diagnostics), is diluted in 80 mL of normal saline and then infused intravenously over 30–60 minutes. Fifteen minutes after completion of Cholografin infusion, CT cholangiogram is acquired through the liver at 1.25 mm slice thickness. Source images are then post-processed for multiplanar reformation and three-dimensional (3D) reconstruction with maximum intensity projection and volume rendering.

MRI has been studied as a sole preoperative imaging modality for potential living liver donor evaluation. In our practice, however, MRI is used as a complementary tool for the evaluation of biliary anatomy when the CT cholangiographic contrast agent, iodipamide meglumin, is not available. To assess biliary anatomy, we acquire both respiratory-trigger 3D T2-weighted magnetic resonance cholangiopancreatography (MRCP) and T1-weighted MRCP at multiple delay time points (15 to 30 minutes delay) following intravenous injection of the hepatobiliary MRI contrast agent Gadoxetate disodium (Eovist, Bayer). The T1-weighted MRCP sequences are gradient recalled echo (GRE) images and performed in a breath-hold.

In the following sections, we will describe the role of CT and MRI in the assessment of liver volumetrics, biliary and hepatic vascular anatomy, and liver parenchyma in potential living liver donors. The impact of the imaging findings on donor selection and surgical planning will be reviewed.

Main points

- Adult living donor liver transplantation (LDLT) is increasingly used for the treatment of end-stage liver disease.
- The decision on which lobe of the liver to harvest for LDLT depends on estimated graft and donor remnant liver volume, as well as biliary and vascular anatomy.
- Awareness of the various anatomic variations and pathologic states, and the impact of such findings on donor selection and surgical planning is essential for the radiologists to generate a meaningful report.

Liver volumetrics

Liver volumetrics is a key component of potential living liver donor evaluation because inadequate liver volume is the most common reason for donor exclusion based on imaging, and the decision to perform left versus right lobe harvesting largely depends on donor liver volume. For the donors, liver remnant volume of 30%–40% of the total liver volume is required for donor survival (7). For the recipients, a graft-to-recipient weight ratio (GRWR) of at least 0.8% or a graft-to-standard liver volume ratio of at least 40% is needed for adequate graft function and to avoid small-for-size syndrome (SFSS) in the recipients (9). SFSS is defined as dysfunction or nonfunction of the graft, characterized by signs of hepatic dysfunction such as cholestasis, ascites, coagulopathy, and encephalopathy, during the first postoperative week after exclusion of other causes. The pathogenesis of SFSS is related to a graft that is too small to meet the demands of the transplant recipient, likely exacerbated by factors such as portal hyperperfusion, poor hepatic venous drainage, steatosis, and poor condition of the patient (high MELD score) (10).

In most patients, the right lobe of the liver is larger and right lobe graft is at much lower risks of SFSS in the transplant recipient. However, right lobe donation is associated with greater donor morbidity and mortality (11). Therefore left lobe donation is preferred for the donors if SFSS can be avoided in the recipient. Additional benefits of using the left lobe include more predictable anatomy and easier anastomosis of the biliary duct, portal venous system, and hepatic venous system (12). A recent study showed that the creation of a hemiportocaval shunt can effectively lower portocaval gradient pressures and may prevent development of SFSS in left lobe grafts with GRWR <0.8% (13).

In contrast, large-for-size grafts generally do not pose as many problems as small-for-size grafts. Problems caused by large-for-size grafts are related to compression in a relatively small abdominal cavity resulting in inadequate blood supply to the graft.

Both CT and MRI can be used to calculate liver volumetrics (Fig. 2). Liver volumes can be determined by manually tracing the contours of the entire liver and the intended graft excluding the large vessels, major fissures and the gallbladder fossa using contiguous CT or MRI images. Recently, automated and semi-automated methods have been put forward that have shown comparable results to the manual methods, and with increased efficiency (14). These automated liver segmentation schemes are based on thresholding, feature analysis, and region growing. When compared with manual methods, the automated methods require substantially less user time, and the liver volumetrics obtained show high concordance with that obtained from manual tracing. Several commercial software packages are available for such liver volumetric calculation. Both CT and MRI have shown equivalent accuracy for liver volume estimation (14). Both modalities, however, tend to overestimate the actual hepatic volume when compared with intra-operative volumetric evaluation, probably due to intra-operative loss of blood (15). Therefore, some authors have proposed the use of conversion factors and formulas to standardize imaging volumetrics (16).

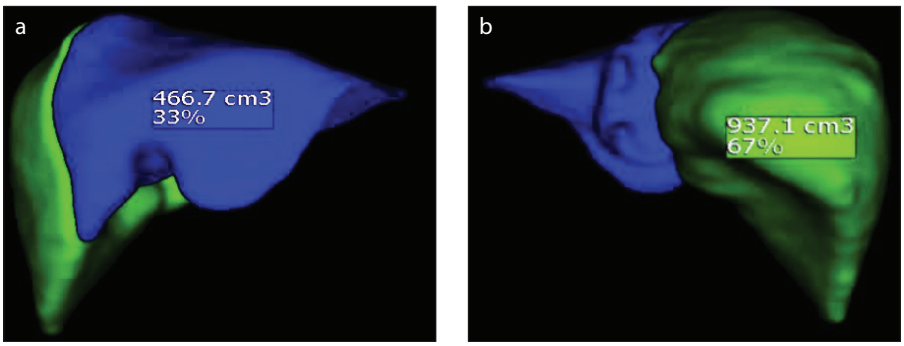

Figure 2. a, b. Three-dimensional (3D) reconstructed CT images demonstrate liver volumetric measurements in cm^3 and % of total liver volume. Depicted are the left *(blue)* and right lobes *(green)* of the liver divided by the hemihepatectomy plane, in the anterior **(a)**, and posterior **(b)** views.

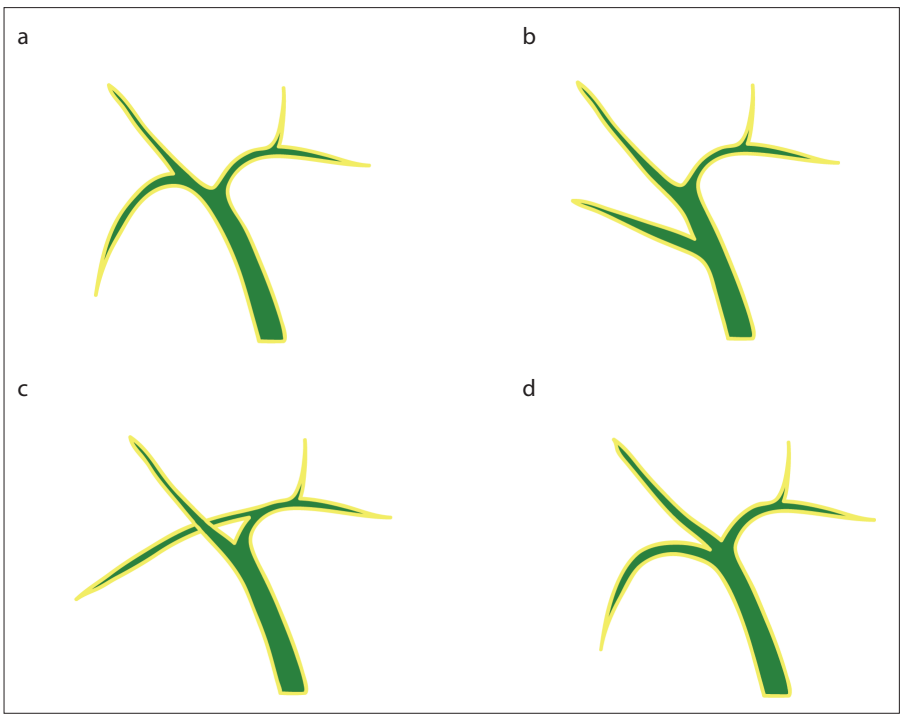

Figure 3. a–d. Schematics of conventional biliary anatomy and three common biliary variants. Conventional biliary anatomy **(a)** occurs in approximately 55% of the population. Right posterior hepatic duct (RPHD) inserting onto common hepatic duct (CHD) **(b)** occurs in approximately 5% of the population. RPHD inserting onto left hepatic duct (LHD) **(c)** occurs in approximately 13%–19% of individuals. Right anterior hepatic duct (RAHD), RPHD, and LHD trifurcating from the CHD **(d)** occurs in approximately 11% of the population.

Biliary imaging

Several schemes, including the Huang classification (17), have been used to classify biliary anatomy. In conventional biliary anatomy, the right posterior hepatic duct (RPHD, draining segments VI and VII) combines with the right anterior hepatic duct (RAHD, draining segments V and VIII) before joining the left hepatic duct (LHD, draining segments II, III, and IV) to become the common hepatic duct (CHD). The ducts draining the caudate lobe may join the left or right hepatic ducts. The cystic duct drains into the CHD below the confluence of right and left hepatic ducts to form the common bile duct. Conventional biliary anatomy is seen approximately in only 55% of people (18). Variant biliary anatomy is more common in the right biliary tree (Fig. 3). In 13%–19% of individuals, the RPHD inserts on the LHD; in 5% of individuals, the RPHD inserts on the CHD; in 11% of individuals, the RPHD, RAHD, and LHD trifurcate from the CHD (19). Biliary complications, such as bile leak and anastomic stricture, are one of the most common causes of morbidity and mortality in LDLT, occurring in the range of 15%–30% (20, 21). Biliary complications are more common when more than one biliary anastomosis is required. Variant biliary anatomy involving right lobe grafts frequently necessitates more than one biliary anastomosis. Therefore accurate preoperative imaging

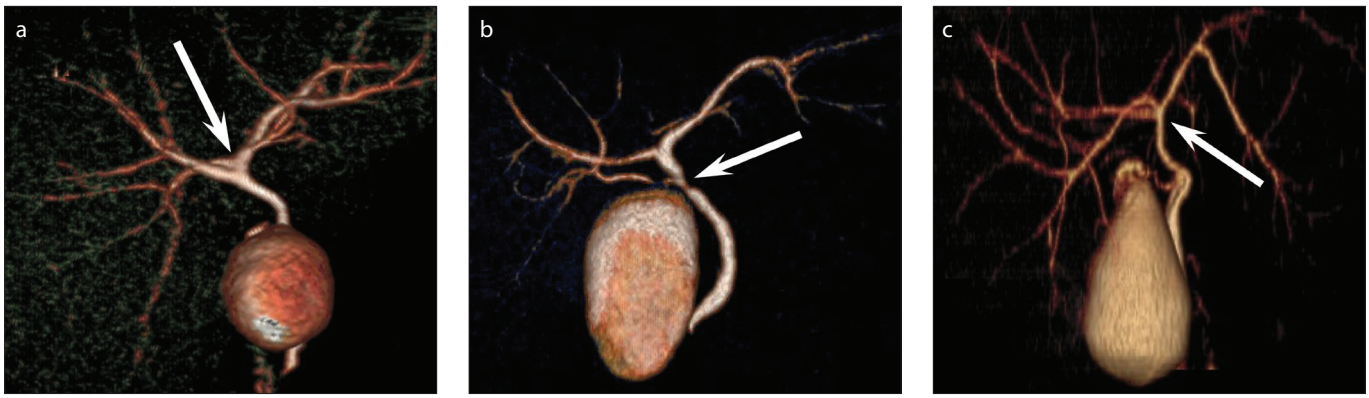

Figure 4. a–c. Variant biliary anatomy shown on volume-rendered CT cholangiograms. Panel **(a)** shows RPHD inserting onto LHD *(arrow)*. Panel **(b)** shows RPHD inserting onto CHD *(arrow)*. Panel **(c)** shows RPHD, RAHD, and LHD trifurcating from the CHD *(arrow)*.

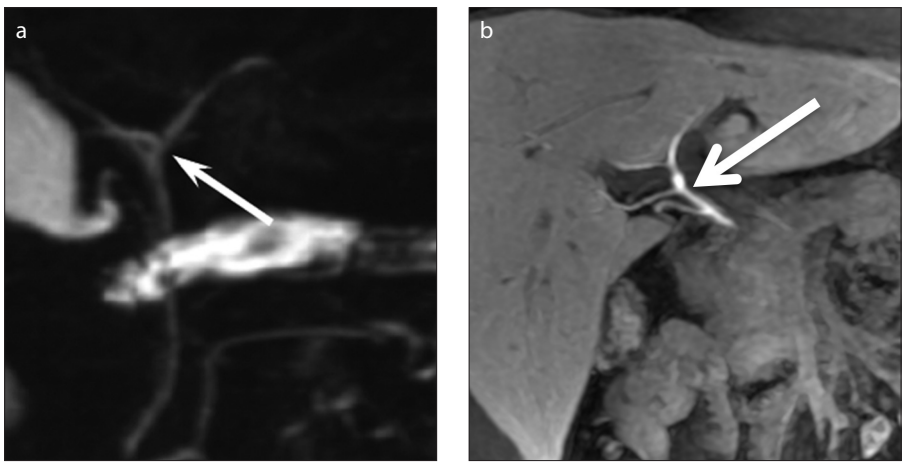

Figure 5. a, b. Biliary variants shown on magnetic resonance cholangiopancreatography (MRCP). Respiratory-triggered thin section 3D T2-weighted MRCP **(a)** shows RPHD inserting onto LHD *(arrow)*. T1-weighted MRCP at 20 minutes delay following intravenous gadoxetate disodium administration **(b)** shows RPHD inserting onto CHD *(arrow)*.

assessment of biliary anatomy is critical for surgical planning and for predicting the risks of biliary complication.

CT cholangiography (CTC) with the cholangiographic contrast agent, iodipamide meglumin, provides an excellent, safe, and minimally invasive option to assess biliary anatomy, risk stratify living liver donors for biliary complications, and aid in preoperative planning. Several studies have shown that CTC enables good-to-excellent visualization of second-order biliary branches (22, 23). Fig. 4 shows examples of CTC depicting variant biliary anatomy in potential living liver donors. Additionally, CTC has been shown to be able to predict biliary complication in the recipients of LDLT. In patients with variant anatomy, the risk of developing biliary complications is much higher if the distance to the corresponding hepatic artery from the second-order bile duct is greater than 1 cm (24). One drawback of CTC is the risk of contrast reactions; however, these occurred at a rate similar to that of conventional contrast-enhanced CT (1%–3%) (25), and no major events were noted, likely reflecting the slower infusion rate of CTC and pre-medication with diphenhydramine (25). Compared with MRCP (discussed below), CTC has higher spatial resolution, shorter scan time, and is less prone to artifact, allowing more consistent visualization of biliary anatomy (26, 27). The use of CTC for LDLT evaluation, however, has not been widespread as the cholangiographic contrast agent iodipamide meglumine is limited in availability.

MRCP is frequently used to depict biliary anatomy in the preoperative evaluation of living liver donors and has shown good accuracy (28). For example, a recent study showed that MRCP has an overall accuracy rate of 91.6%, with 84.9% sensitivity, 96% specificity, 88.2% positive predictive value, and 94.7% negative predictive value, when compared with intraoperative cholangiogram (28). An advantage of MRCP over CTC is its lack of ionizing radiation; an important consideration for living liver donors who tend to be relatively young and may receive multiple follow-up scans. A key sequence for MRI biliary evaluation is a high quality respiratory-triggered thin slice 3D T2-weighted MRCP sequence. In a recent study of 20 patients, 3D T2-weighted MRCP accurately predicted biliary anatomy in 18 patients, with 100% positive predictive value and specificity for normal biliary anatomy (29). Fig. 5a shows an example of variant biliary anatomy depicted on a T2-weighted MRCP image. Another key MRI sequence for biliary evaluation is a T1-weighted MRCP following intravenous administration of hepatobiliary contrast agents, such as gadoxetate disodium (Eovist, Bayer). Typically, 50% of the gadoxetate disodium is taken up by hepatocytes to be excreted into the bile, and the biliary anatomy is best depicted between 20–120 min after injection (30). Fig. 5b shows example of biliary variant depicted on 20 minutes delay T1-weighted MRCP following gadoxetate disodium administration. Various sequence modifications can optimize results. In particular, an increased flip angle can improve contrast between the biliary tree, radial k-space sampling can minimize motion artifacts, and free-breathing acquisition can improve signal-to-noise ratio (31). In addition, intravenous low-dose morphine has been shown to distend and improve bile duct visualization in gadoxetate disodium enhanced MRCP (32).

Hepatic vascular imaging

Hepatic arterial anatomy can be classified using the Michel classification (33). In conventional hepatic arterial anatomy, the right and left hepatic arteries (RHA, LHA) arise from the proper hepatic artery, a

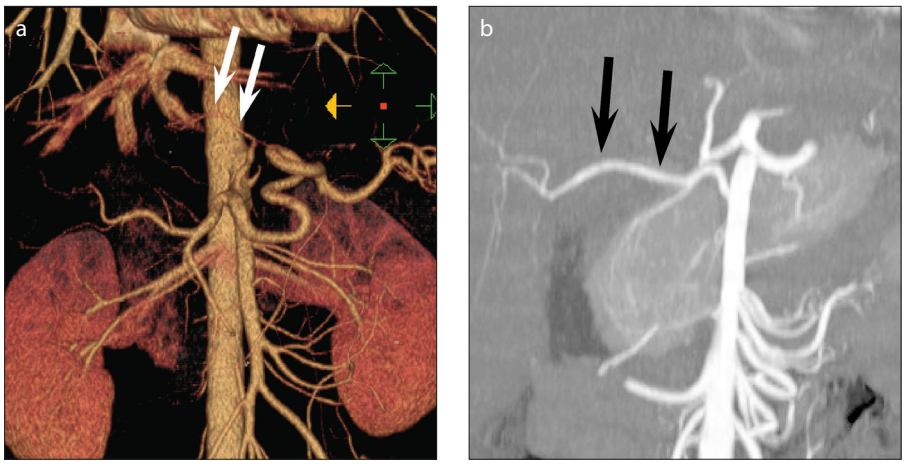

Figure 6. a, b. Hepatic arterial variants shown on CT angiograms. Volume-rendered image **(a)** shows a left accessory hepatic artery *(arrows)* arising from the left gastric artery. Maximum intensity projection (MIP) image **(b)** shows a replaced right hepatic artery *(arrows)* from the superior mesenteric artery.

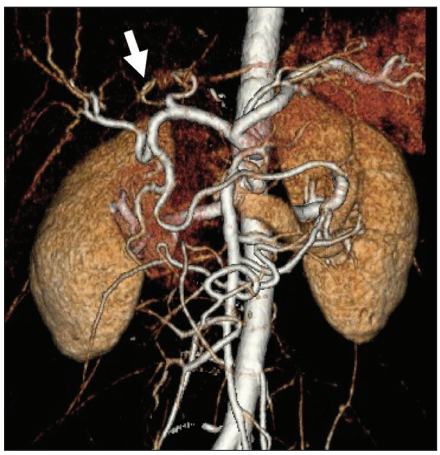

Figure 7. Segment IV hepatic artery shown on CT angiogram. Volume rendered image shows segment IV hepatic artery *(arrow)* arising from the left hepatic artery.

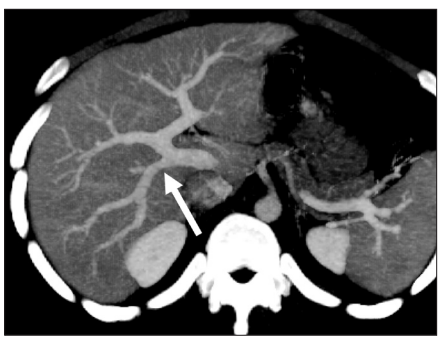

Figure 8. Portal vein variant shown on CT angiogram. MIP image demonstrates a direct origin of the right posterior portal vein from the main portal vein *(arrow)*.

branch of the common hepatic artery (CHA) beyond the origin of the gastroduodenal artery. Such conventional anatomy occurs in approximately only 55% of the population (34). Common variants include a replaced or accessory LHA (from the left gastric artery, 18%) and a replaced or accessory RHA (from the superior mesenteric artery, 18%) (19) (Fig. 6). Accurate preoperative assessment for such variants is necessary for surgical planning and reducing risks of graft ischemia and biliary complications. A hepatic arterial variant to note is the origin of the segment IV artery, sometimes referred to as the middle hepatic artery. Segment IV artery can arise either from the LHA or the RHA (Fig. 7). For right lobe graft harvesting, it is mandatory to preserve the segment IV artery to ensure adequate regeneration of the residual liver in the donor. In left lobe graft harvesting, segment IV artery arising from RHA will require two anastomoses: one for the LHA and another one for the segment IV artery.

Conventional portal venous anatomy consists of the main portal vein dividing into the right and left portal veins. The right portal vein then further divides into anterior and posterior branches. Portal venous variants account for approximately 20% of all significant vascular variants (35). Important variants to note on preoperative imaging include trifurcation of the main portal vein into right anterior and posterior portal vein branches and left portal vein, and direct origin of the right posterior portal vein from the main portal vein (Fig. 8). Knowledge of such variants is important for surgical planning. For example, in a right lobe graft, direct origin of the right posterior portal vein from the main portal vein or the trifurcation of the main portal vein would necessitate two portal vein anastomoses, which also increase the risk of postoperative portal vein thrombosis (36).

Conventional hepatic venous anatomy consists of the right (RHV; draining segments V-VII), middle (MHV; draining segments IV, V, and VIII), and left (LHV; draining segments II and III) hepatic veins draining separately into the IVC. In 60% of patients, the MHV and LHV join before draining into the IVC (34). Segment I, or the caudate lobe, usually has a separate drainage into the IVC. Detailed hepatic venous mapping is important as the plane of donor hepatectomies is determined by the anatomy of the hepatic veins. Typically, hemihepatectomies are performed along the Cantlie's line along the gallbladder fossa, which lies 1 cm to the right of the MHV (Fig. 1). In general, any vessels that run through this transection plane are prone to injury during surgery. For example, in right donor hepatectomy, the presence of large branching veins draining into MHV from the right lobe (Fig. 9) may necessitate alteration of the transection plane, and/or separate anastomosis of the venous branches to IVC to avoid venous congestion (37). It is also important to identify any accessory inferior right hepatic veins that drain directly into the IVC. Accessory hepatic veins with a diameter of 5 mm or more will require separate anastomoses to the IVC to prevent hepatic congestions. A distance of 4 cm or more in the coronal plane between the accessory vein and the confluence of the hepatic veins (Fig. 10) may make it difficult to surgically implant both veins with a single occluding clamp on the recipient's IVC (38).

For potential living liver donor vascular evaluation, CT angiography (CTA) is the most commonly used modality with comparable results to, and without the invasiveness, cost, or radiation exposure of traditional angiography. Its high spatial resolution and excellent contrast between vessels and surrounding parenchyma allow detection of a wide range of vascular variants that may affect surgical planning or are relative contraindications to LDLT (39). Magnetic resonance angiography using a gadolinium-based agent with bolus tracking has also been used extensively for vascular imaging. It is safe, noninvasive, and radiation-free. However, it has longer scan time and is more prone to motion artifacts (19), and therefore small vessels may not be consistently visualized on magnetic resonance angiography.

Liver parenchyma imaging

Diffuse parenchymal liver disease poses risks for both the donor and recipient in LDLT. In particular, nonalcoholic fatty liver

disease is the most common parenchymal pathology found in potential living liver donors. There is a higher prevalence of nonalcoholic fatty liver disease among men, and patients with obesity, type 2 diabetes, and hyperlipidemia (40). A recent study showed that the presence of more than 30% of macrovesicular steatosis was an independent risk factor for impaired one-year graft survival (41). Therefore detection of significant fatty liver is a critical component of potential living liver donor evaluation.

CT and MRI are the most commonly used imaging modalities for noninvasive detection of fatty liver (42). Unenhanced CT is a simple method to estimate the degree of fatty liver (Fig. 11). Studies have shown that the finding of liver attenuation more than 10 Hounsfield units (HUs) lower than that of the spleen has 88%–95% sensitivity and 90%–99% specificity for the diagnosis of 30% or greater steatosis in the liver (43). In addition, an absolute HU of 40 or less has been reported to represent at least 30% fatty liver (44). A hepatic-to-splenic attenuation ratio of 0.8 or less has been shown to have 100% specificity for 30% or greater fatty liver (45). Administration of contrast interferes with the CT method of fatty liver quantification. Dual-echo chemical shift MRI has also been used extensively in the clinics to detect the presence of fatty liver (46). Loss of signal on out-of-phase images suggests fatty liver. A previous study showed that normal and fatty liver were correctly differentiated with chemical shift out-of-phase and in-phase imaging in 68%–93% of cases (47). Proton density fat fraction calculation is a recently described chemical-shift-based water and fat separation technique (iterative decomposition of water and fat with echo asymmetry and least squares estimation, IDEAL-IQ) that can be completed in a breath-hold and allows for simple calculation of liver fat fraction (Fig. 12). The advantage of this technique is that it provides correction of factors that influence MRI signal intensity, such as T1 bias, and T2* decay. This technique has been shown to provide accurate quantification of hepatic fat content in potential living liver donors (48).

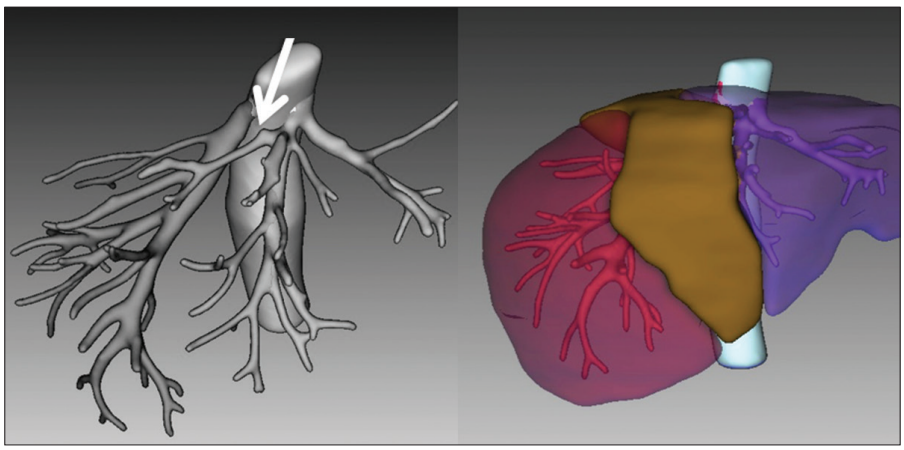

Figure 9. Large branching vein draining into the middle hepatic vein. **Left:** A 3D reconstructed image from a CT angiogram demonstrates a large vein *(arrow)* draining the right lobe into the middle hepatic vein. **Right:** The corresponding paramedian sector of the right liver lobe *(brown)* that is drained by the branching vein of the middle hepatic vein.

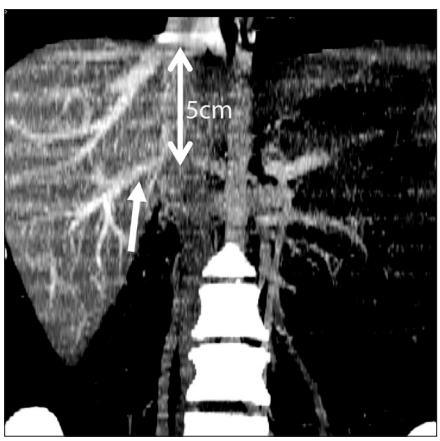

Figure 10. Hepatic vein variant shown on CT angiogram. MIP image demonstrates an accessory inferior right hepatic vein *(arrow)* that drains directly into the IVC. The distance between accessory vein and the confluence of the hepatic veins is 5 cm in the coronal plane.

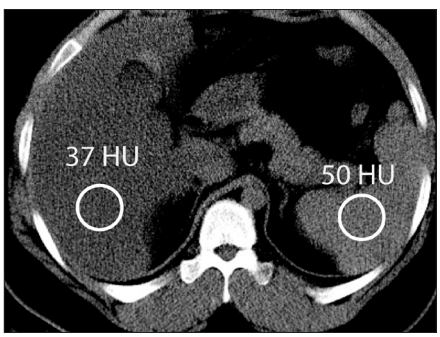

Figure 11. Unenhanced axial CT of the upper abdomen demonstrates diffuse fatty liver. The liver attenuation is 37 HU, which is >10 HU lower than that of the spleen.

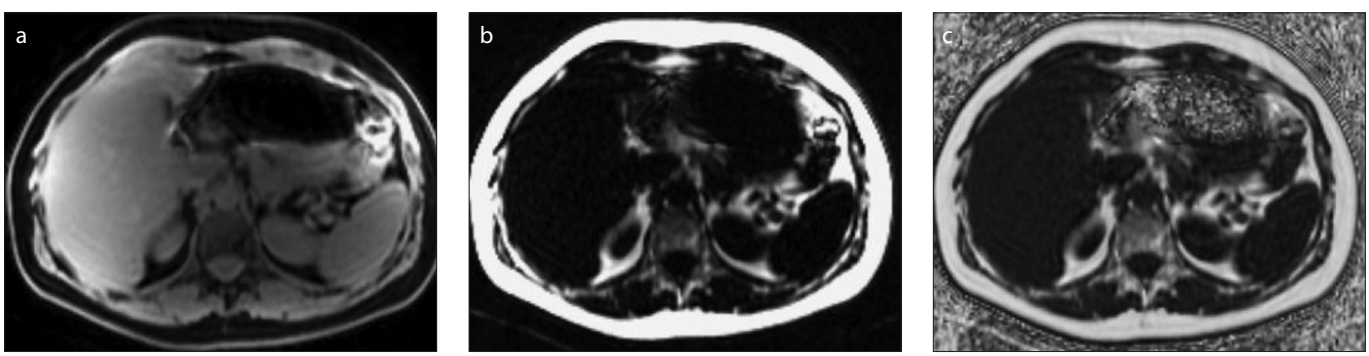

Figure 12. a–c. Liver fat quantification using the chemical-shift-based water and fat separation technique (iterative decomposition of water and fat with echo asymmetry and least squares estimation, IDEAL-IQ). Panels show water image **(a)**, fat image **(b)**, and T2* corrected proton density fat fraction (PDFF) image **(c)**. The mean fat fraction is 4% in this liver donor.

Through the use of CT and MRI, various focal liver lesions may be detected in living liver donors (49). Findings suggestive of malignancy, such as hepatocellular carcinoma or metastases, will preclude living liver donation. Other benign lesions, such as cysts, hemangiomas, or focal nodular hyperplasia, depending on their size and location, may also affect the risk for both donor and recipient in LDLT. These findings should be reported to the surgeon to help risk stratify living liver donors.

Conclusion

CT and MRI are key imaging modalities that allow for a noninvasive and comprehensive evaluation of potential living liver donors, including the assessment of liver volumetrics, biliary and hepatic vascular anatomy, and liver parenchyma. Awareness of the various anatomic variations and pathologic states, and the impact of such findings on donor selection and surgical planning is essential for the radiologists to generate a meaningful report and to become an integral part of the LDLT team.

Conflict of interest disclosure

The authors declared no conflicts of interest.

References

1. Hoehn R, Wilson G, Wima K, et al. Comparing living donor and deceased donor liver transplantation: A matched national analysis from 2007 to 2012. Liver Transpl 2014; 20:1347–1355. [CrossRef]
2. Bhatti A, Zia H, Dar F, et al. Quality of life after living donor hepatectomy for liver transplantation. World J Surg 2015; 39:2300–2305. [CrossRef]
3. Kolthoff K, Merion R, Ghobrial R, et al. Outcomes of 385 adult-to-adult living donor liver transplant recipients. A report from the A2ALL consortium. Ann Surg 2005; 242:314–325.
4. Ladner D, Dew M, Forney S, et al. Long-term quality of life after liver donation in the adult to adult living donor liver transplantation cohort study (A2ALL). J Hepatol 2015; 62:346–353. [CrossRef]
5. Suh K, Suh S, Lee J, Choi Y, Yi N, Lee K. Recent advancements in and views on the donor operation in living donor liver transplantation: a single-center study of 886 patients over 13 years. Liver Transpl 2015; 21:329–338. [CrossRef]
6. Muzaale AD, Dagher NN, Montgomery RA, Taranto SE, McBride MA, Segev DL. Estimates of early death, acute liver failure, and long-term mortality among live liver donors. Gastroenterology 2012; 142:273–280. [CrossRef]
7. Makuuchi M, Sugawara Y. Technical progress in living donor liver transplantation for adults. HPB (Oxford) 2004; 6:95–98. [CrossRef]
8. Hahn L, Emre S, Israel G. Radiographic features of potential donor livers that precluded donation. AJR Am J Roentgenol 2014; 202:W343–348. [CrossRef]
9. Lo CM, Fan ST, Liu CL, et al. Adult-to-adult living donor liver transplantation using extended right lobe grafts. Ann Surg 1997; 226:261–270. [CrossRef]
10. Dahm F, Georgiev P, Clavien P. Small-for-size syndrome after partial liver transplantation: definition, mechanisms of disease and clinical implications. Am J Transplant 2005; 5:2605–2610. [CrossRef]
11. Taketomi A, Kayashima H, Soejima Y, et al. Donor risk in adult-to-adult living donor liver transplantation: impact of left lobe graft. Transplantation 2009; 87:445–450. [CrossRef]
12. Sudhindran S, Menon R, Balakrishnan D. Challenges and outcome of left-lobe liver transplants in adult living donor liver transplants. J Clin Exp Hepatol 2012; 2:181–187. [CrossRef]
13. Botha J, Langnas A, Campos B, et al. Left lobe adult-to-adult living donor liver transplantation: small grafts and hemiportocaval shunts in the prevention of small-for-size syndrome. Liver Transpl 2010; 16:649–657. [CrossRef]
14. D'Onofrio M, De Robertis R, Demozzi E, Crosara S, Canestrini S, Pozzi Mucelli R. Liver volumetry: Is imaging reliable? Personal experience and review of the literature. World J Radiol 2014; 6:62–71. [CrossRef]
15. Niehues SM, Unger JK, Malinowski M, Neymeyer J, Hamm B, Stockmann M. Liver volume measurement: reason of the difference between in vivo CT-volumetry and intraoperative ex vivo determination and how to cope it. Eur J Med Res 2010; 15:345–350. [CrossRef]
16. Karlo C, Reiner CS, Stolzmann P, et al. CT- and MRI-based volumetry of resected liver specimen: comparison to intraoperative volume and weight measurements and calculation of conversion factors. Eur J Radiol 2010; 75:e107–111. [CrossRef]
17. Huang TL, Cheng YF, Chen CL, Chen TY, Lee TY. Variants of the bile ducts: clinical application in the potential donor of living-related hepatic transplantation. Transplant Proc 1996; 28:1669–1670.
18. Mortele KJ, Ros PR. Anatomic variants of the biliary tree: MR cholangiographic findings and clinical applications. AJR Am J Roentgenol 2001; 177:389–394. [CrossRef]
19. Catalano O, Singh A, Uppot R, Hahn P, Ferrone C, Sahani D. Vascular and biliary variants in the liver: implications for liver surgery. Radiographics 2008; 28. [CrossRef]
20. Brown RS, Jr., Russo MW, Lai M, et al. A survey of liver transplantation from living adult donors in the United States. N Engl J Med 2003; 348:818–825. [CrossRef]
21. Hampe T, Dogan A, Encke J, et al. Biliary complications after liver transplantation. Clin Transplant 2006; 20 Suppl 17:93–96. [CrossRef]
22. Wang Z, Yeh B, Roberts J, Breiman R, Qayyum A, Coakley F. Living donor candidates for right hepatic lobe transplantation: evaluation at CT cholangiography--initial experience. Radiology 2005; 235:899–904. [CrossRef]
23. McSweeney SE, Kim TK, Jang HJ, Khalili K. Biliary anatomy in potential right hepatic lobe living donor liver transplantation (LDLT): the utility of CT cholangiography in the setting of inconclusive MRCP. Eur J Radiol 2012; 81:6–12. [CrossRef]
24. Yeh B, Coakley F, Westphalen A, et al. Predicting biliary complications in right lobe liver transplant recipients according to distance between donor's bile duct and corresponding hepatic artery. Radiology 2007; 242:144–151. [CrossRef]
25. Van Beers B, Lacrosse M, Trigaux J, Canniere L, De Ronde T, Pringot J. Noninvasive imaging of the biliary tree before or after laparoscopic cholecystectomy: use of three-dimensional spiral CT cholangiography. AJR Am J Roentgenol 1994; 162:1331–1335. [CrossRef]
26. Yeh B, Breiman R, Taouli B, Qayyum A, Roberts J, Coakley F. Biliary tract depiction in living potential liver donors: comparison of conventional MR, mangafodipir trisodium-enhanced excretory MR, and multi-detector row CT cholangiography--initial experience. Radiology 2004; 230:645–651. [CrossRef]
27. McSweeney S, Kim T, Jang H, Khalili K. Biliary anatomy in potential right hepatic lobe living donor liver transplantation (LDLT): the utility of CT cholangiography in the setting of inconclusive MRCP. Eur J Radiol 2012; 81:6–12. [CrossRef]
28. Hsu H, Tsang L, Yap A, et al. Magnetic resonance cholangiography in living donor liver transplantation. Transplantation 2011; 92:94–99. [CrossRef]
29. Ragab A, Lopez-Soler R, Oto A, Testa G. Correlation between 3D-MRCP and intra-operative findings in right liver donors. Hepatobiliary Surg Nutr 2013; 2:7–13.
30. Frydrychowicz A, Lubner M, Brown J, et al. Hepatobiliary MR Imaging with Gadolinium Based Contrast Agents. J Magn Reson Imaging 2012; 35:492–511. [CrossRef]
31. Rosenkrantz A, TK B, Hindman N, Vega E, Chandarana H. Combination of increased flip angle, radial k-space trajectory, and free breathing acquisition for improved detection of a biliary variant at living donor liver transplant evaluation using gadoxetic acid-enhanced MRCP. J Comput Assist Tomogr 2014; 38:277–280. [CrossRef]
32. Agrawal M, Mennitt K, Zhang H, et al. Morphine three-dimensional T1 gadoxetate MR cholangiography of potential living related liver donors. J Magn Reson Imaging 2014; 39:584–589. [CrossRef]
33. Covey AM, Brody LA, Maluccio MA, Getrajdman GI, Brown KT. Variant hepatic arterial anatomy revisited: digital subtraction angiography performed in 600 patients. Radiology 2002; 224:542–547. [CrossRef]
34. Sahani D, Mehta A, Blake M, Prasad S, Harris G, Saini S. Preoperative hepatic vascular evaluation with CT and MR angiography: implications for surgery. Radiographics 2004; 24:1367–1380. [CrossRef]
35. Cheng Y, Huang T, Lee T, Chen T, Chen C. Variation of the intrahepatic portal vein; angiographic demonstration and application in living-related hepatic transplantation. Transplant Proc 1996;28:1667–1668.
36. Kamel IR, Kruskal JB, Pomfret EA, Keogan MT, Warmbrand G, Raptopoulos V. Impact of multidetector CT on donor selection and surgical planning before living adult right lobe liver transplantation. AJR Am J Roentgenol 2001; 176:193–200. [CrossRef]
37. Kamel I, Lawler J, Fishman E. Variations in anatomy of the middle hepatic vein and their impact on formal right hepatectomy. Abdom Imaging 2003; 28:668–674. [CrossRef]
38. Erbay N, Raptopoulos V, Pomfret E, Kamel I, Kruskal J. Living donor liver transplantation in adults: vascular variants important in surgical planning for donors and recipients. AJR Am J Roentgenol 2003; 181:109–114. [CrossRef]

39. Guiney M, Kruskai J, Sosna J, Hanto D, Goldberg S, Raptopoulos V. Multi-detector row CT of relevant vascular anatomy of the surgical plane in split-liver transplantation. Radiology 2003; 229:401–407. [CrossRef]
40. Adams L, Lymp J, St Sauver J, et al. The natural history of nonalcoholic fatty liver disease: a population-based cohort study. Gastroenterology 2005; 129:113–121. [CrossRef]
41. Spitzer AL, Lao OB, Dick AA, et al. The biopsied donor liver: incorporating macrosteatosis into high-risk donor assessment. Liver Transpl 2010; 16:874–884. [CrossRef]
42. Cheng Y, Yu C, Ou H, et al. Section 1. Image evaluation of fatty liver in living donor liver transplantation. Transplantation 2014; 97(Suppl 8):S3–6. [CrossRef]
43. Lee S, Park S, Kim K, et al. Unenhanced CT for assessment of macrovesicular hepatic steatosis in living liver donors: comparison of visual grading with liver attenuation index. Radiology 2007; 244:479–485. [CrossRef]
44. Kodama Y, CS N, Wu T, et al. Comparison of CT methods for determining the fat content of the liver. AJR Am J Roentgenol 2007; 188:1307–1312. [CrossRef]
45. Park S, Kim P, Kim K, et al. Macrovesicular hepatic steatosis in living liver donors: use of CT for quantitative and qualitative assessment. Radiology 2006; 239:105–112. [CrossRef]
46. Pilleul F, Chave G, Dumortier J, Scoazec J, Valette P. Fatty infiltration of the liver. Detection and grading using dual T1 gradient echo sequences on clinical MR system. Gastroenterol Clin Biol 2005; 29:1143–1147. [CrossRef]
47. Kim H, Taksali SE, Dufour S, et al. Comparative MR study of hepatic fat quantification using single-voxel proton spectroscopy, two-point dixon and three-point IDEAL. Magn Reson Med 2008; 59:521–527. [CrossRef]
48. Chiang H, Lin L, Li C, et al. Magnetic resonance fat quantification in living donor liver transplantation. Transplant Proc 2014; 46:666–668. [CrossRef]
49. Ringe K, Husarik D, Sirlin C, Merkle E. Gadoxetate disodium-enhanced MRI of the liver: part 1, protocol optimization and lesion appearance in the noncirrhotic liver. AJR Am J Roentgenol 2010; 195:13–28. [CrossRef]